Numerical Simulations of a Mechanically-Ventilated Multi-Compartment Fire

TAREK BEJI[1], FREDERICK BONTE[2], and BART MERCI[1]
[1]Department of Flow, Heat and Combustion Mechanics
Ghent University
Sint-Pietersnieuwstraat 41, Ghent, Belgium
[2]Bel V
Rue Walcourt 148, Anderlecht, Belgium

ABSTRACT

The objective of this work was to evaluate the capabilities of a widely used Computational Fluid Dynamics (CFD) code in the fire community, namely the Fire Dynamics Simulator (FDS 5.5.3), in the simulation of a large-scale, well-confined and mechanically ventilated multi-room fire scenario. The CFD analysis focuses on the effect of pressure build-up induced by the fire on the ventilation network. The measured heat release rate (HRR) was therefore prescribed as input in the simulations. Computational results were compared to measurements obtained for one of several experimental scenarios performed at the French Institut de Radioprotection et de Sûreté Nucléaire (IRSN). The overall trend was well reproduced by FDS. Quantitative comparisons for respectively the total relative pressure, ventilation flow rates and gas temperature (in the fire room) at the steady-state combustion regime have shown underestimations of 18 to 22 %.

KEYWORDS: compartment fires, forced ventilation, Computational Fluid Dynamics (CFD), Fire Dynamics Simulator (FDS).

NOMENCLATURE LISTING

$\dot{m}$	mass flow rate (kg/s)	*in*	inflow
N_{cells}	number of cells	*max*	maximum fan value
T	temperature (°C)	*out*	outflow
t	time (s)	o_2	oxygen
$\dot{V}$	volume flow rate (m^3/s or m^3/h)	*u*	upper layer
p	pressure (Pa)	*0*	initial value
Greek		**superscript**	
Δp	pressure difference (Pa)	*exp*	experimental
Δx	mesh size (cm)	*c*	corridor
ε^{exp}	experimental uncertainty (%)	*num*	numerical
ε	deviation between exp. and num. (%)	*1*	room 1
ρ	density (kg/m^3)	*2*	room 2
χ	molar concentration (mol/mol)	*3*	room 3
subscripts		$\bar{}$	background pressure
a	ambient		pressure perturbation

INTRODUCTION

In order to improve the understanding of fire-related phenomena in nuclear facilities, a large international collaborative research program, named the PRISME project, has been initiated in December 2006 [1]. The French acronym PRISME stands for "Fire Propagation in Elementary Multi-Room Scenarios". The project relies on extensive experimental testing in conjunction with a fire modelling analysis for a wide range of fire scenarios. The experimental campaigns are carried out at the French Institut de Radioprotection et de Sûreté Nucléaire (IRSN) facilities in Cadarache, France [1]. Fire modelling capabilities are examined and assessed within the analytical working group of PRISME using a set of several fire modelling codes in a number of benchmark exercises [2].

In the performed experimental tests a number of aspects are addressed. The first one is related to the characterization of several potential fire sources in a nuclear facility, such as liquid pools of Hydrogenated

Tetra Propylene (HTP) (a solvent similar to Dodecane and used for reprocessing) [3] or electrical cabinets (made of transformers, circuit breakers, cable trays,…etc) [4]. Such characterization is first undertaken in free-burn conditions (*i.e.* open atmosphere) by monitoring the mass loss rate (MLR) and the heat release rate (HRR). The latter is measured using the Oxygen Consumption (OC) and/or the Carbon Dioxide Generation (CDG) technique [3]. The second aspect is related to the interaction of the mechanical ventilation with the fire in a well confined compartment. These effects are quantified and examined in terms of induced MLRs (and subsequent HRRs) [5-7], room pressure variations and changing ventilation flow rates for several initial renewal rates (*i.e.* volumetric flow rates divided by the volume of the enclosure) [8]. Other pressure-related effects such as leakages were also addressed. Finally, smoke and heat spread in the multi-compartment configuration (e.g. [6, 9]) is examined for up to 5 compartments (*i.e.* 4 rooms and 1 corridor) connected by vertical openings (*i.e.* doorways) and/or horizontal ones with varying fire sources and operating ventilation conditions. The set of 5 compartments is called the DIVA facility.
Many fire phenomena cited above (*e.g.* characterization of fire sources or multi-compartment effects and doorway flows) are not specific to the nuclear safety industry and a large body of literature is devoted to these problems. In this work we have chosen to address and focus on the issue of the interaction of the ventilation network with the fire-induced pressure build-up in a confined facility. This is typically encountered in the nuclear industry where the ventilation network ensures, in normal operating conditions, dynamic confinement in order to contain the potential release of radioactive material and avoid dispersion to the outside [8]. The analysis of experimental data [8] has shown that, in the event of a fire, overpressures of more than 2500 Pa can occur within the fire room in conjunction with a substantial change in the operating conditions of the ventilation network. These changes include for instance the back flow (or flow inversion) a phenomenon, which means that inlet ducts may act as outlet. Therefore, in a Fire Hazard Analysis (FHA) two major consequences must be taken into account: the loss of dynamic confinement and the possible mechanical damage of safety devices [8].
The decision making process regarding fire safety assessment in nuclear installations depends increasingly on computer simulations. Given the wide variety of available computer codes a systematic validation process is required for each code in order to identify its strengths and weaknesses, as well as the level of uncertainty in the results produced. The benchmark exercise presented in [2] shows that, for a specified scenario, deviations between measurements and numerical results vary over a wide range of values, depending on the code as well as the user. For instance, in [2], eight simulations using the Fire Dynamics Simulator (FDS) produced global errors in the mean temperature between 8 and 35 %. These deviations are not only due to the use of different versions of FDS. The results obtained by 2 different users of the same version of FDS showed deviations of 10 and 24 %. This is referred to as the "user-effect".
When simulating fire scenarios similar to the one considered in this work there are mainly three options available in FDS:

1- The first option consists of prescribing fixed boundary conditions at the inlet and outlet ducts using the initial volume flow rates.
2- The second option consists of defining pressure zones and simulating the pressure-related effects of the fans located at the inlet and outlet ducts of the multi-compartment facility.
3- The third option consists of simulating the full ventilation network, which means not only the fans located at the inlet and outlet ducts of the multi-compartment facility but also the complete set of branches, pipes and fans placed downstream (*e.g.*[10]).

In the work presented here, our first objective is to evaluate FDS 5.5.3 [11] for a specific scenario as part of a benchmark exercise. We intend to explain in detail the set-up and main features of the numerical model in order to minimize the "user-effect" for future calculations. More specifically, we considered option 2 in our calculations for two reasons. Firstly, we ruled out option 1 because fire-induced pressure profiles and changing ventilation flow rates are not simulated in this case. Secondly, option 3 requires the set-up of a complete and complex Heat Ventilation and Air Conditioning (HVAC) system, which might lead to increased computational times and uncertainties. The latter are not necessarily reduced in comparison with option 2. It is important to mention that although a newer version of FDS (FDS 6) [12] is in the pre-release phase, the results obtained here remain up-to-date because the features used in FDS 5.5.3 are still present in FDS 6. It is true that FDS 6 offers more possibilities regarding the modelling of a complete and complex HVAC system. However, we deliberately opt for a simpler approach in the present study for the reasons cited above.

EXPERIMENTAL SET-UP AND DETAILS

The geometry of the multi-compartment set-up consists of three rooms (room 1 to 3) and a corridor (see Fig.1). Each room is 6 m long, 5 m wide and 4 m high. The corridor is 15.6 m long, 2.5 m wide and 4 m high. Walls are made of concrete with a thickness of 0.3 m. In all four compartments the ceiling is protected with 50 mm-thick insulating rock-wool panels. Additionally, in room 2 (*i.e.* the fire room), the four walls are insulated with rock-wool panels, 60 mm-thick on the upper part and 30 mm-thick on the lower part. Room 3 is thermally protected with 30 mm-thick rock-wool panels on the four walls. Floors of the four compartments are not insulated. Natural ventilation is provided through three doorways between rooms 1 and 2, 2 and 3 and room 2 and the corridor. The doorways are centered on the corresponding separating wall. The dimensions are 2.10 m × 0.81 m for room1-room2 and room2-room3 doorways and 2.10 m × 0.86 m for the room2-corridor doorway.

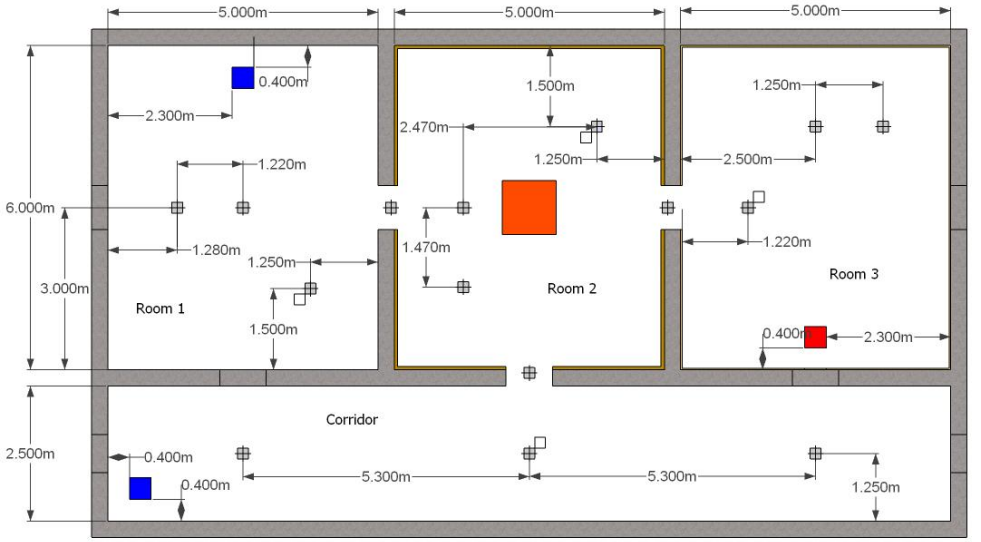

Fig. 1. Plan view of the multi-compartment facility (to scale) showing the inlet (in blue) and outlet (in red) ducts. The centered-burner in room 2 is circular in the experiment but drawn here as square, similarly to the FDS model. The solid and open squares indicate respectively thermocouple trees and gas analyzers.

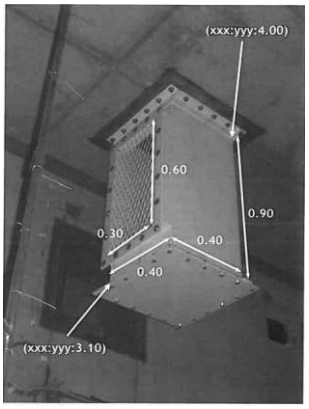

Fig. 2. Inlet and outlet openings in the DIVA facility (courtesy of IRSN).

The mechanical ventilation network consists of two inlet ducts in the upper part of room 1 and the corridor and a single outlet duct in the upper part of room 3. The air inlet and outlet openings have a cross section of 0.18 m^2 (0.3 m × 0.6 m) and they are at 3.1 m from the floor (see Fig.2). The locations of the ducts in each compartment are presented in Fig. 1. The initial volumetric flow rates at the inlet and outlet ducts are measured. Besides, the ventilation network is composed of 13 additional nodes in order to ensure dynamic confinement between the DIVA facility (initially at pressure p_0 < 0 Pa) and the open atmosphere. The

ventilation flow rates and pressures in each node are measured but only the information already provided in this section will be used for the numerical simulations described here. The fire source is a $1m^2$ HTP pool fire (the pan diameter is 1.129 m) located at the centre of room 2, 0.4 m above floor level.
A highly dense instrumentation with more than 500 sensors has been set up to monitor the fire. The instrumentation includes: (1) gas analyzers, (2) particle analyzers, (3) pressure transducers, (4) thermocouples, (5) heat flux meters, (6) bidirectional velocity probes, (7) tachymeters, (8) flow meters and (9) video cameras. For the sake of clarity and due to space limitations, only the positions of the thermocouple trees and the gas analyzers are shown in Fig. 1.

NUMERICAL MODEL

In this section, the main features of FDS (5.5.3) are briefly described first. Then, a detailed description of the mechanical ventilation system set-up and the pressure-related effects is provided. Finally, additional numerical details are given before providing a list of the simulations performed.

Brief description of FDS

As mentioned earlier, the CFD package used in this work is FDS 5.5.3 [10]. FDS has been developed by the National Institute of Standards and Technology (NIST) for fire-driven flows. The Navier-Stokes equations are solved using second order finite differences numerical scheme with a low Mach number formulation. The main combustion model is based on the mixture fraction concept with infinitely fast chemistry. The turbulence model is based on Large Eddy Simulation (LES). The Radiative Transfer Equation (RTE) is solved using the Finite Volume Method (FVM). A radiative fraction is prescribed (by default) as an upper bound in order to limit the uncertainties in the radiation calculation induced by uncertainties in the temperature field. In this simulation, the default value of 0.35 was kept for HTP. Heat losses to the walls are computed by solving the 1-D Fourier's equation for conduction. As for the fire source, FDS offers the possibility to model pool fires including the complex phenomena of heat-up, vaporization and burning of liquid fuel. However, due to the uncertainties, which still remain in the modelling of these phenomena, the measured heat release rate was prescribed as input in FDS. Furthermore, the default constants in FDS were not changed. The focus in this paper is on the ventilation network and the pressure-related effects, which will be discussed in the following section.

Set-up of the mechanical ventilation

In the event of a fire in well-confined and mechanically ventilated compartments, pressure-related effects have a substantial influence on the level of ventilation ensured by the fans, which extract vitiated air and inject fresh air. The basic FDS equation set assumes pressure to be composed of a "background" component, $\bar{p}\ z,t$, plus a perturbation, $\tilde{p}\ x,t$ [10]. The former is the hydrostatic pressure. The latter is the flow-induced pressure calculated by FDS at each time step.
In order to simulate a flow between two volumes at different pressures, each volume must be defined as a "pressure zone" having its own background pressure. In addition to that, the set-up a full HVAC system as proposed in FDS 6 requires a number of parameters such as the lengths of ducts to be defined. In the configuration considered here, setting up the full ventilation network (with 16 nodes and the associated pressures and volume flow rates) is a tedious task that requires a lot of information to be prescribed and processed in the numerical model, which leads to a substantial increase in the required computational times. As mentioned earlier, the problem is simplified in this work with the objective of evaluating to what extent such a simplification is reliable. Two pressure zones are defined. The first one covers the 4 compartments (3 rooms and the corridor). Although it is expected to have some differences in the pressure between the 4 compartments, since they are connected by three doors, the four volumes are assumed to have one background pressure. Experimental results confirm the validity of this assumption for the complete duration of the fire. The transient pressure profiles measured in room 1, room 3 and corridor are similar. The set of four compartments is connected to the surrounding environment. The latter is considered as a separate zone which is always at ambient pressure.
The initial pressure, P_0, in the 4 compartments is negative and within a range of 20 Pa. In the simulations performed here, ambient pressure is taken as initial condition (*i.e.* $p_0 = 0$ Pa). Therefore, in order to be able to compare the results, overpressures (*i.e.* $\Delta p = p\text{-}p_0$) will be considered as previously done in [8]. An essential component of the system is the fan. In FDS [10], the volume flow supplied by a fan is given by:

$$\dot{V} = \dot{V}_{\max} \cdot sign\ \left(\Delta p_{\max} - \Delta p\right) \cdot \sqrt{\frac{\left|\Delta p - \Delta p_{\max}\right|}{\Delta p_{\max}}} \qquad (1)$$

where $\dot{V}$ is the volume flow rate of the fan, $\dot{V}_{\max}$ its maximum volume flow rate, Δp the pressure difference between two zones and Δp_{max} the maximum operating pressure of the fan.

Figure 3 shows the curves corresponding to Eq. (1) for two fans. The first fan (Fig. 3a) is placed in an inlet duct and the second fan (Fig. 3b) in an outlet duct. The initial operating conditions are taken at null static pressure and $\Delta p_{\max}$ = 1000 Pa. Figure 3a shows that the pressure build-up induced by a fire will cause a reduction in the air inflow until $\Delta p = 1000\,Pa$ where it becomes zero. For pressures beyond 1000 Pa the flow is inversed, *i.e.* the inlet duct acts as an outlet duct which extracts smoke. On the contrary, the outlet duct acts during the whole duration of the fire as an outlet with an increasing volume flow as the pressure increases (see Fig. 3b). In Fig. 3, it is taken by convention that a positive (resp. negative) volume flow rate corresponds to air inlet (resp. outlet).

In the experiments, the initial operating conditions of the fans are provided in terms of volume flow rates for the given initial pressure. Since in the modelling we made the choice of starting from ambient conditions instead of reconstructing the entire ventilation network and the corresponding pressures, we only consider the initial measured values as V_{max} values. The remaining unknown is $\Delta p_{\max}$, the maximum operating pressure of the fan. This information is not readily available. Furthermore, it must not be seen in this case as an intrinsic property of each fan since it will depend on the interaction with the other fans placed downstream, which are not incorporated in the model. Therefore, in order to examine the uncertainty related to this issue, a sensitivity study is performed on $\Delta p_{\max}$ by considering three values: 500 Pa, 1000 Pa and 1500 Pa. For the sake of simplicity, the geometry shown in Fig. 2 was not exactly reproduced. Instead, openings of 0.40 m by 0.40 m were set in the ceiling at the locations given in Fig. 1.

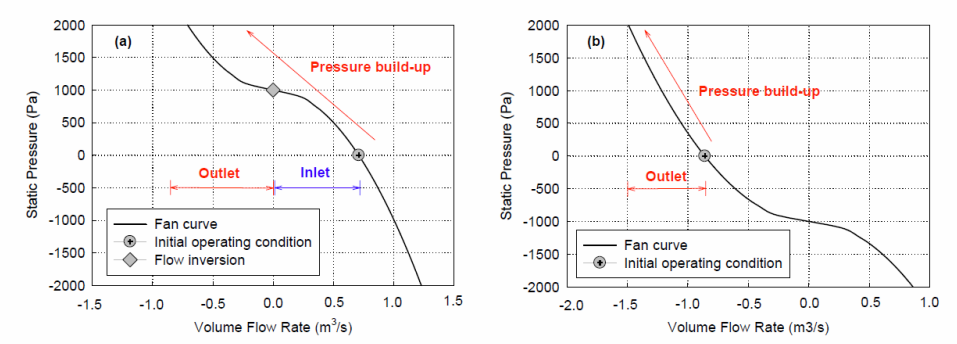

Fig. 3. Example of two fan curves using the quadratic fan model of FDS: (a) Inlet and (b) Outlet.

In addition to volume flows supplied by fans, FDS offers the possibility to simulate volume flows through leakages. However, experimental measurements have shown that the DIVA facility is very tight. Therefore, the contribution of leakages is neglected here (similarly to the analysis of the experimental data provided in [8]).

Numerical details and list of simulations

The domain considered in FDS was slightly extended on the sides and more importantly by 2 m in the vertical position in order to resolve well the smoke flow at the exhaust duct. A structured uniform mesh was used for all simulations. The mesh size was 20 cm in 3 simulations and 10 cm in one simulation in order to evaluate its effect on the results. The number of cells can be written in the three directions in the form of $2^n \times 3^m \times 5^l$ as suggested in [10] in order to optimize the calculations of the Poisson pressure solver. A summary of the simulation details is provided in Table 1. It is important to note that, in order to have stabilized initial flow conditions, a period of 1 minute has been included before activating the fire.

Table 1. List of simulations.

Sim_ID	Δp_{max} (Pa)	Δx (cm)	N_{cells}
S1	1000	20	100×64×30 = 192,000
S1'	1000	10	180×120×60 = 1,296,000
S2	1500	20	100×64×30 = 192,000
S3	500	20	100×64×30 = 192,000

RESULTS AND DISCUSSION

For confidentiality reasons, the experimental results are not shown in terms of absolute values. The focus is on the deviation between experimental and numerical results.

General trend

Figure 4 shows that, as expected, the FDS HRR output reproduces the overall trend prescribed as input. This trend shows 4 distinct phases:

1. In the first unsteady phase, the HRR increases and then falls to its nominal value. During this phase, the changing operating conditions of the ventilation network and the subsequent pressure profile are qualitatively well reproduced (see Fig.5a). The fire induced pressure increase results in a decrease in volume flow rate of fresh air as supplied by the inlet ducts in room 1 and in the corridor (see Figs. 5b-c). The flow inversion time is numerically well predicted. Then, for a given period of time, both inlet ducts act as exhaust ducts (see Figs. 5b-c). The conjunction of this event with the continuous extraction of smoke by the outlet duct in room 3 causes the pressure to decrease and stabilize after having reached a peak of around 1000 Pa. Figures 6 and 7 show that the temperature and smoke layer height profiles are reasonably well predicted during this phase.
2. During the quasi-steady state period, an equilibrium situation is established in the ventilation conditions. The pressure and HRR profiles fluctuate around a quasi-steady state value. However, numerically predicted extraction and inflow rates yield a higher steady-state pressure in the well-confined structure (see Fig. 5a). Furthermore, the subsequent predicted lower amounts of oxygen supplied result in a lower HRR and an underestimation of the temperature in the fire room by more than 20%. The results of the quasi-steady state will be analyzed in more detail in the next sub-section.
3. A second peak in the HRR and pressure was measured. This second peak can be explained by a heat flux exerted over a thinner layer of liquid, increasing therefore the evaporation and the burning rates. Similarly to the steady-state phase, not enough oxygen is brought into the enclosure and the peak HRR is not reproduced. This leads to a substantial temperature prediction, particularly in the fire room (see Fig. 7).
4. Decay phase: Despite the imposed extinction of the fire in the FDS input HRR, sustained burning is observed (see Fig. 4), particularly at the exhaust where hot gases reach ambient oxygen concentrations. More details about this phenomenon will be addressed in the next section since it is a consequence of the previously established steady-state stage.

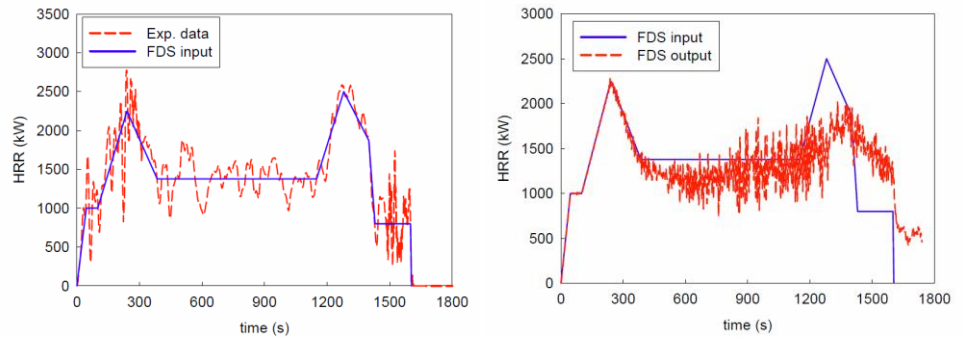

Fig. 4. HRR profiles: experimental measurement, FDS input and FDS output.

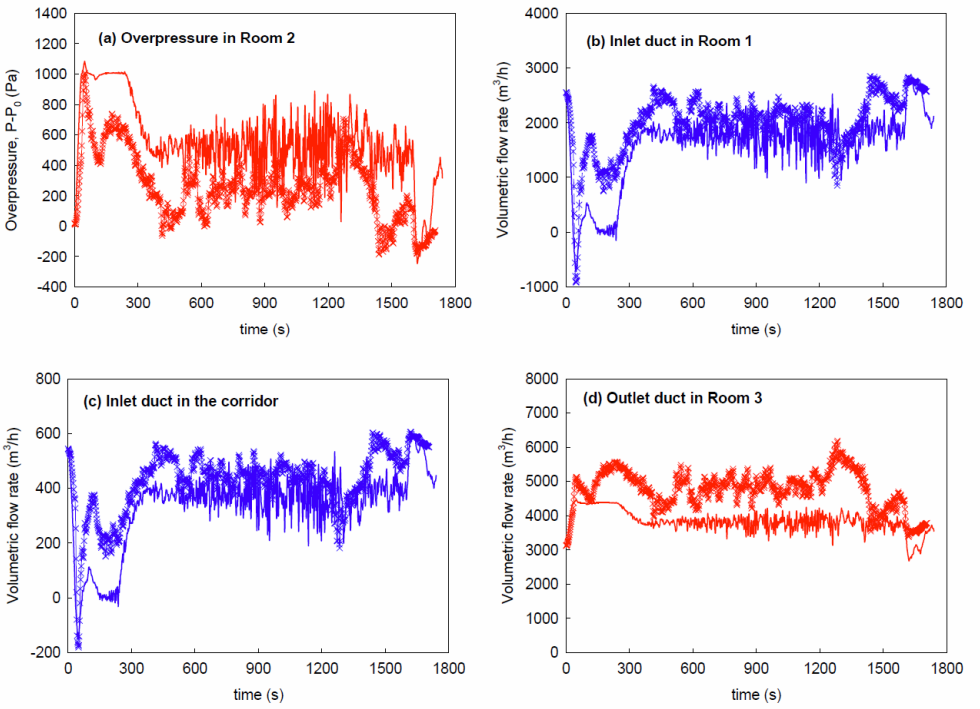

Fig. 5. Comparison between experimental (symbols) and numerical data (lines) for simulation S1: (a) the overpressure in room 2, (b) inflow volume flow rate in room 1, (c) inflow flow rate in the corridor, and (d) outflow volume flow rate in room 3.

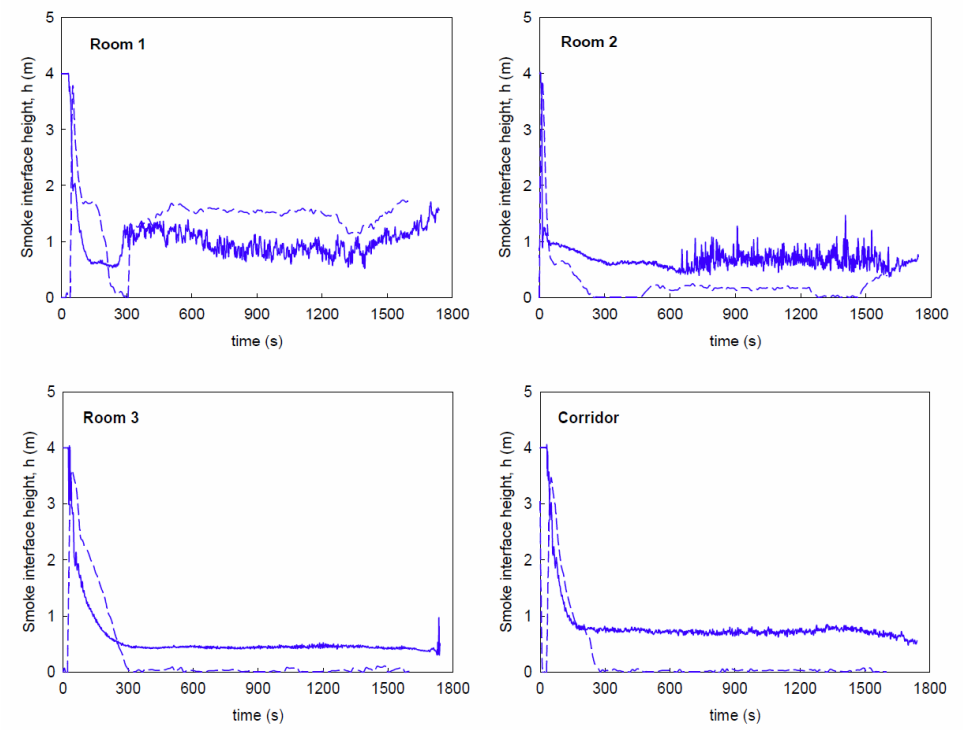

Fig. 6. Comparison between experimental (dashed) and numerical data (solid) for simulation S1 for the smoke interface height profiles in the four compartments.

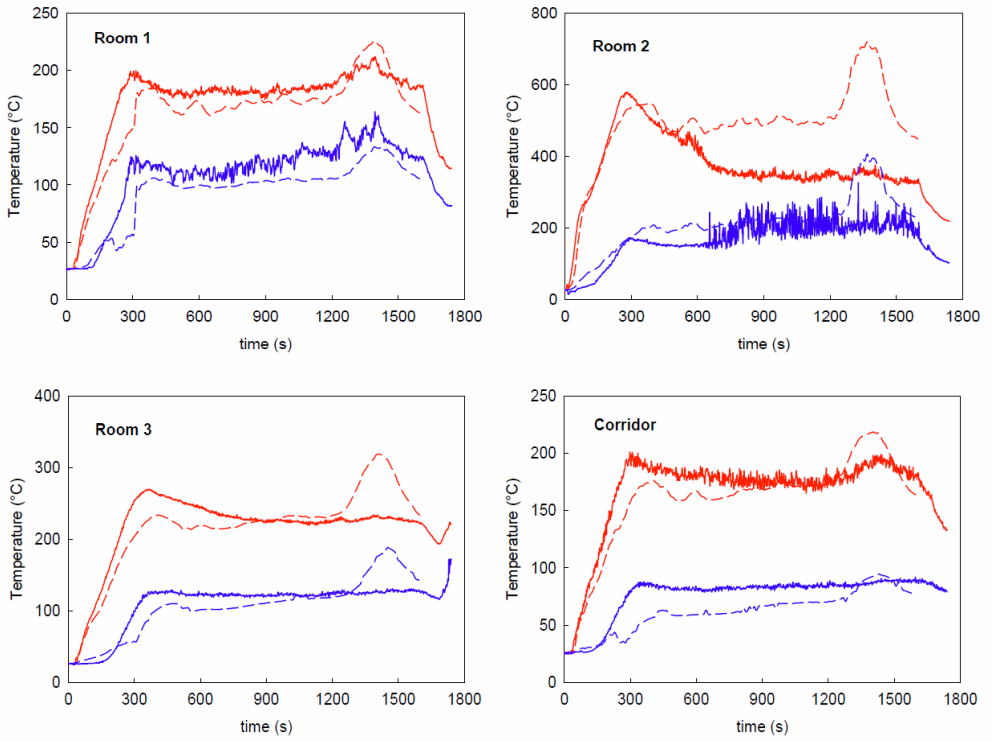

Fig. 7. Comparison between experimental (dashed) and numerical data (solid) for simulation S1 for the upper layer and lower layer temperature profiles in the four compartments.

The smoke layer interface and the layer temperatures have been numerically calculated in FDS using the method developed in [13].

Steady-state stage

The steady-stage is examined in more detail here. Table 2 displays a comparison between the experimental and numerical results at this stage. An indication of experimental uncertainties, ε^{exp}, for pressure, volume flow rates, oxygen concentration and temperature was provided in [2]. Prétrel et al. [8] pointed out that it is difficult to evaluate the experimental uncertainty in HRR measurements. However, they noted possible significant differences between the OC and the CDG methods, the latter considered as more appropriate for configurations similar to the one at hand. The deviation, ε, between experimental and numerical results for a quantity ϕ is given by:

$$\varepsilon = \left(\frac{\phi^{num} - \phi^{\exp}}{\phi^{\exp}} \right) \times 100 \qquad (2)$$

The numerical results indicate that:

- Refining the mesh size from 20 cm to 10 cm does not change the results. Thus, a mesh size of 20 cm is considered as appropriate for the purposes of this work.
- The value of Δp_{max} (500, 1000 or 1500 Pa) has an influence only on the predicted overpressure, the value of 500 Pa in simulation S3 yielding the best agreement in terms of Δp (ε = 22.1 % < ε_{exp} = ± 30 %). The other results for S1, S2 and S3 are almost identical.

In order to visualize the agreement between the experimental data and the numerical results, deviations higher than experimental uncertainties are highlighted in grey in Table 2. Except for the difference in Δp (which was commented upon above), all the numerical results show a significant underestimation (between 18 and 22%) in the predictions of the volume flow rates (at the inlet and outlet ducts) and the upper layer temperature in the fire room. This could be explained by the fact that the ventilation set-up in the numerical

model did not provide sufficient oxygen levels within the fire room to reproduce the HRR measured in the experiments and provided as input in FDS.
By considering the multi-compartment structure as a control volume, the global mass balance for oxygen at the steady-state stage reads:

$$\dot{m}_{O_2,in} = \chi_{O_2}^1 \dot{V}_{in}^1 + \chi_{O_2}^c \dot{V}_{in}^c \rho_a - \chi_{O_2}^3 \dot{V}_{out}^3 \rho_u^3 \quad (3)$$

where $\dot{m}_{O_2}$ (kg/s) is the oxygen mass flow rate, χ_{O_2} (mol/mol) the oxygen volume fraction , $\dot{V}$ (m^3/s) the volume flow rate, ρ_a (kg/m^3) the ambient air density and ρ_u (kg/m^3) the upper layer density. The subscripts *in* and *out* represent respectively the inflow and outflow of air at the inlet and outlet ducts. The superscripts 1, *c* and 3 indicate respectively room 1, the corridor and room 3.
Applying Eq. (3) to respectively the experimental and numerical data yields a numerical under-prediction of 12.6 %. This explains the HRR under-predictions (see Table 2) because the fire is ventilation-controlled. Figure 8 shows that, at some point during the steady-state stage, the flame detaches from the burner surface and some burning takes place outside the fire room. Figure 8 shows also that, at the exhaust (in room 3), when hot gases with low oxygen levels are in contact with fresh air, a continuous burning takes place. These numerical results are in accordance with the model incorporated in FDS, which separates the burning from the non-burning zone as a function of oxygen volume fraction and temperature [11]. As a consequence of a lower HRR predicted in the fire room, the steady-state upper layer temperature in the fire room is under-predicted by about 22 %.
In order to confirm that the main problem is due to ventilation, a complementary simulation has been performed. In this simulation, only the steady-state stage is considered with a HRR corresponding to the average experimental HRR. Pressure effects are ignored and the fans are not modeled. Instead, a fixed volumetric flow rate was prescribed as a boundary condition at the duct openings. The values assigned were the measured experimental data at the steady-state stage.

Table 2. Comparison of experimental and numerical results for the steady-state stage.

	Exp.		**S1**		**S1'**		**S2**		**S3**	
	Val.	ε^{exp} **(%)**	**Val.**	**ε (%)**	**Val.**	**ε (%)**	**Val.**	**ε (%)**	**Val.**	**ε (%)**
HRR (kW)	1377	-	1121	-18.6	1175	-14.7	1223	-11.2	1220	-11.4
Δp (Pa)	208	± 30	503	141.8	514	147.1	705	238.9	254	22.1
$\dot{V}_{in}^1$ (m^3/s)	0.602	± 10	0.496	-17.6	0.489	-18.8	0.496	-17.6	0.493	-18.1
$\dot{V}_{in}^c$ (m^3/s)	0.128	± 10	0.105	-18.0	0.103	-19.5	0.105	-18.0	0.104	-18.8
$\dot{V}_{out}^3$ (m^3/s)	1.323	± 10	1.054	-20.3	1.055	-20.3	1.055	-20.3	1.050	-20.6
$\chi_{O_2}^1$ (mol/mol)	0.208	± 2	0.209	0.5	0.209	0.5	0.209	0.5	0.209	0.5
$\chi_{O_2}^c$ (mol/mol)	0.208	± 2	0.209	0.5	0.209	0.5	0.209	0.5	0.209	0.5
$\chi_{O_2}^3$ (mol/mol)	0.098	± 2	0.099	1.0	0.102	4.1	0.099	1.0	0.099	1.0
T_u^1 (°C)	171	± 10	182	6.4	182	6.4	182	6.4	181	5.9
T_u^2 (°C)	493	± 10	384	-22.1	382	-22.5	387	-21.5	383	-22.3
T_u^3 (°C)	224	± 10	236	5.4	235	4.9	236	5.4	235	1.9
T_u^c (°C)	167	± 10	178	6.6	174	4.2	179	7.2	178	6.6

As expected, a better agreement is obtained for the predicted temperature in the fire room. The predicted value is within a range of less than 1% from the experimental measurement.

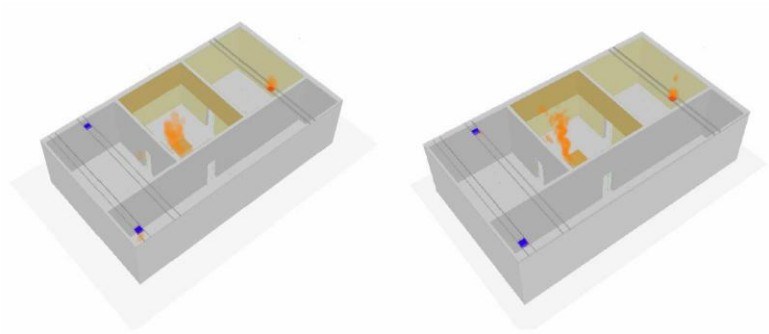

(a) (b)

Fig. 8. Smokeview 3-D visualization of the flame in FDS at 300 s after ignition: (a) S1, (b) S1'.

CONCLUSIONS

Numerical simulations using FDS (5.5.3) were carried out for a mechanically-ventilated multi-compartment fire in the framework of a benchmark exercise within the PRISME project. Such a configuration is particularly relevant for the nuclear industry where a forced-ventilation network is set up to ensure dynamic confinement and prevent the release of radioactive material to the outside. The main purpose was to focus on the assessment of the current capabilities of FDS (5.5.3) to simulate the ventilation conditions and their interaction with the fire. Therefore, the measured HRR was prescribed as input in FDS. In the methodology proposed here, the full ventilation network (with the total number of nodes) is not simulated. Only the fans at the inlet and outlet ducts are modeled including the pressure-related effects. The main outcomes of the performed simulations are the following:

- For the case considered (and similar cases), a mesh size of 20 cm is sufficient to examine the ventilation and pressure profiles and their interaction with the fire. A finer mesh of 10 cm does not provide any additional qualitative or quantitative insight.
- In addition to the initial volume flow rates (which are usually known), the definition of the operating conditions of the fans requires the set of a maximum operating pressure, which is not readily obtainable. The sensitivity analysis performed here has shown that the value of 500 Pa gives the best agreement in terms of overpressure in the compartments. The other quantities such as volume flow rates and hot gas temperatures do not change by modifying the maximum operating pressure of the fans.
- The global trend is well reproduced by FDS for the pressure, volume flow rates and temperatures. This trend includes the prediction of the back flow phenomenon at the inlet ducts when the overpressure exceeds the operating pressure of the fans.
- The overall level of ventilation was under-predicted by FDS for the studied case. The inflow rate of oxygen during the steady-state region was under-predicted by around 12.6 %, leading to a lower predicted HRR and therefore lower upper layer temperature in the fire room by 22 %.

It appears that FDS (5.5.3) can give a good first basis for a fire hazard analysis in forced-ventilated enclosure fires provided that the HRR is known from experiments or design calculation requirements. The main limitation lies in the under-ventilated steady-state stage where the level of ventilation is under-estimated. In addition to the evaluation of FDS 5.5.3, the simulations performed here will provide valuable information to assess the new capabilities and the added value offered by FDS 6 in its pre-release version. The new capabilities include the set-up of the full ventilation network and the simulation of air flow at each node of the system.

ACKNOWLEDGMENTS

This research was funded by Bel V in the framework of cooperation with Ghent University (contract Ref. number A12/TT/0617).

REFERENCES

[1] Rigollet, L., Noterman, N., Gorza, E., Siccama, A., Peco, J., Ito, T., Röwekamp, M., Bounagui, A., Lamarre, G., Gay, L., Audouin, L., Gonzalez, R., Prétrel, H., and Suard, S., "Application of the OECD PRISME results to investigate heat and smoke propagation mechanism in multi-compartment fire scenarios," Organisation for Economic Co-operation and Development (OECD) Report NEA/CSNI/R(2012)14, 2012, 39 p.

[2] Audouin, L., Chandra, L., Consalvi, J.L., Gay, L., Gorza, E., Hohm, V., Hostikka, S., Ito, T., Klein-Hessling, W., Lallemand, C., Magnusson, T., Noterman, N., Park, J.S., Peco, J., Rigollet, L., Suard, S., and Van-Hees, P., (2011) Quantifying Differences Between Computational Results and Measurements in the Case of a Large-Scale Well-Confined Fire Scenario, Nuclear Engineering and Design 241:18-31. http://dx.doi.org/10.1016/j.nucengdes.2010.10.027.

[3] Prétrel, H., Le Saux, W., and Audouin, L., (2013) Determination of the Heat Release Rate of Large Scale Hydrocarbon Pool Fires in Ventilated Compartments, Fire Safety Journal (in press, corrected proof). http://dx.doi.org/10.1016/j.firesaf.2013.01.014.

[4] Coutin, M., Plumecoq, W., Melis, S., and Audouin, L., (2012) Energy Balance in a Confined Fire Compartment to Assess the Heat Release Rate of an Electrical Cabinet Fire, Fire Safety Journal 52:34-45. http://dx.doi.org/10.1016/j.firesaf.2012.05.002.

[5] Prétrel, H., Querre, P., and Forestier, M., "Experimental Study of Burning Rate Behaviour in Confined and Ventilated Fire Compartments," *Fire Safety Science -- Proceedings of the eight International Symposium*, International Association for Fire Safety Science, 2005, pp. 1217-1228. http://dx.doi.org/10.3801/IAFSS.FSS.8-1217

[6] Le Saux, W., Prétrel, H., Lucchesi, C., and Guillou, P., "Experimental Study of the Fire Mass Loss Rate in Confined and Mechanically Ventilated Compartment Fires," *Fire Safety Science -- Proceedings of the ninth International Symposium*, International Association for Fire Safety Science, 2008, pp. 943-954. http://dx.doi.org/10.3801/IAFSS.FSS.9-943

[7] Melis, S., and Audouin, L., "Effects of Vitiation on the Heat Release Rate in Mechanically-Ventilated Compartment Fires," *Fire Safety Science -- Proceedings of the ninth International Symposium*, International Association for Fire Safety Science, 2008, pp. 931-942. http://dx.doi.org/10.3801/IAFSS.FSS.9-931

[8] Prétrel, H., Le Saux, W., and Audouin, L., (2012) Pressure Variations Induced by a Pool Fire in a Well-Confined and Force-Ventilated Compartment, Fire Safety Journal 52:11-24.

[9] Prétrel, H., and Audouin, L., "Doorway Flows Induced by the Combined Effects of Natural and Forced Ventilation in a Three Compartment Assembly," *Fire Safety Science -- Proceedings of the ninth International Symposium*, International Association for Fire Safety Science, 2011, pp. 1015-1027. http://dx.doi.org/10.3801/IAFSS.FSS.10-1015

[10] Bonte, F., Noterman, N., and Merci, B.,(2013) Computer Simulations to Study Interaction Between Burning Rates and Pressure Variations in confined Enclosure Fires, Fire Safety Journal. http://dx.doi.org/10.1016/j.firesaf.2013.01.030.

[11] McGrattan, K., Klein, B., Hostikka, S., and Floyd, J., "Fire Dynamics Simulator (Version 5) User's Guide," National Institute of Standards and Technology Report NIST Special Publication 1019-5, Gaithersburg, MD, 2009, 176 p.

[12] McGrattan, K., Klein, B., Hostikka, S., and Floyd, J., "Fire Dynamics Simulator (Version 6) User's Guide," National Institute of Standards and Technology Report NIST Special Publication 1019, Gaithersburg, MD, 2012.

[13] Janssens, M.L., Tran, H.C., (1992) Data Reduction of Room Tests for Zone Model Validation, Journal of Fire Sciences 10:528-555. http://dx.doi.org/10.1177/073490419201000604.